Drought Recurrence and Seasonal Rainfall Prediction in the Río Yaqui Basin, Mexico

Robert E. Nicholas and David S. Battisti

Department of Atmospheric Sciences
University of Washington, Seattle, Washington

corresponding author:

Robert E. Nicholas
Department of Atmospheric Sciences
University of Washington, Box 351640
Seattle, WA 98195-1640

rnicholas@atmos.washington.edu

ABSTRACT

A statistical approach is used to explore the variability of precipitation and meteorological drought in Mexico's Río Yaqui basin on seasonal-to-decadal timescales. For this purpose, a number of custom datasets have been developed, including a monthly 1900-2004 precipitation index for the Yaqui basin created by merging two gridded land-surface precipitation products, a 350-year tree-ring based proxy for Yaqui wintertime rainfall, and a variety of large-scale climate indices derived from gridded SST records. Although significantly more rain falls during the summer (JJAS) than during the winter (NDJFMA), wintertime rainfall is over three times as variable relative to the climatological mean. Summertime rainfall appears to be unrelated to any large-scale patterns of variability but a strong relationship between ENSO and Yaqui rainfall during the winter months offers the possibility of meaningful statistical prediction for this season's precipitation. Analysis of both historical and reconstructed rainfall data suggests that meteorological droughts as severe as the 1994-2002 Yaqui drought occur about twice per century, droughts of even greater severity have occurred in the past, and such droughts are generally associated with wintertime anomalies. While summertime reservoir inflow is larger in the Yaqui basin, wintertime inflow is more variable (in both relative and absolute terms) and is much more strongly correlated with same-season rainfall. Using the identified wintertime ENSO-rainfall relationship, two simple empirical forecast models for possible use by irrigation planners are demonstrated.

1. Introduction

a. Geographic, agricultural, and social context

Covering 79,172 km^2 (World Resources Institute 1998), the Río Yaqui watershed lies primarily in the Mexican state of Sonora, extending eastward into Chihuahua and northward into southern Arizona (Figure 1). The Yaqui drains the western slopes of the Sierra Madre Occidental into the Gulf of California near the city of Obregón and constitutes one of the major river systems of northwest Mexico.

Although the Yaqui basin is characterized by a semi-arid climate (and in the east, rather mountainous terrain), it is nonetheless an extraordinarily important agricultural region. Three major reservoirs, completed in the 1940s and 1960s, provide water for irrigation of fertile farmlands in the lower Yaqui Valley. This highly productive agricultural region was an early home of the so-called Green Revolution through which scientific management and increased use of fertilizers, pesticides, and hybrid cultivars led to dramatic increases in crop yields during the latter half of the 20th century. Durum wheat production anchors a local agricultural economy that also includes maize, safflower, soy, hay, hogs, cattle, vegetable crops, and, most recently, shrimp aquaculture. Wheat yields (in metric tons per hectare) over the past thirty years have averaged more than double the average yield for North and Central America (McCullough 2005), and the Yaqui region is responsible for nearly two-fifths of Mexico's annual wheat production (Lobell et al. 2005b). Finally, grazing is important in the uncultivated scrublands of the region.

b. Recent drought

Because of its use of stored water for irrigation, the Yaqui agricultural economy is mostly resilient to short-term precipitation deficits; however, this state of affairs leaves it especially vulnerable to disruption by multi-year drought. A recent drought, extending from 1994 into 2002, highlighted this vulnerability. Although crop yields initially increased due to lower nighttime minimum temperatures caused by reduced cloud cover (Lobell et al. 2005, Fischer 1985), the reservoirs eventually emptied, leading to dramatically reduced yields. At the height of the drought, only about one-fifth of the farmland in the normally-productive Yaqui Irrigation District was cultivated. Although 2003 brought above-normal rainfall that helped replenish the dessicated reservoir system, questions of vulnerability to drought and long-term sustainability remain as the most recent winter (2006) has brought a return to dry conditions.

c. Questions to be addressed in this paper

Although motivated by concerns that are agricultural and economic, the focus of this work is on the meteorology and climate (particularly with regard to precipitation) of the Yaqui region. As such, the subsequent analysis and discussion is guided by the following questions:

- How does precipitation "work" in the Yaqui basin? What is the annual cycle of precipitation? What are the key sources of variability?

- What is the relationship between precipitation and reservoir storage? Does this relationship vary with season?

- Is there a particular seasonality associated with drought? What large scale climatic patterns, if any, are associated with severe droughts and pluvials?

- How severe was the most recent drought? How does it compare to previous droughts?

- Can this knowledge be used to make skillful and useful predictions of seasonal rainfall for the Yaqui basin?

- What can the past tell us about what to expect in the future?

Agricultural or hydrological droughts may be associated with anomalies in a variety of quantities, including groundwater levels and surface evaporation. However, we will show that, in this region, extended periods of water deficit for agricultural applications are mainly associated with wintertime precipitation anomalies. Hence, throughout this paper, the term "drought" is taken to mean sustained deficits in rainfall (a more precise definition is offered in section 5a). Unless otherwise noted, the period of record is water years 1901-2004 (October 1900 through September 2004) and we have required that all statistical quantities (e.g. correlation coefficients) exceed the 95% confidence level ($p = 0.05$) to be considered statistically significant.

2. Data

Because one of the goals of this study is to explore variability in Yaqui precipitation at long timescales (e.g. droughts that may last from several years to more than a decade), we have sought to obtain the longest possible precipitation record that would also encompass the most recent drought. Although we have found no single record matching both of these criteria, by extending a portion of the 1900-1996 Hulme et al. (1998) dataset with precipitation from the 1925-2004 dataset of Zhu and Lettenmaier (2007), we were able to produce a single "merged" index of Yaqui precipitation for water years 1901-2004. This index is a measure of average rainfall over the entire "Yaqui region" defined by the two Hulme gridboxes marked with dashed lines in Figure 1, rather than simply an average of precipitation records within the Yaqui watershed itself, where the station network is sparse and local records may contain significant gaps. Unless otherwise noted, the terms "Yaqui rainfall," "Yaqui precipitation," "Yaqui basin," and "instrumental record" refer to this outlined region, 26.25°-31.25°N and 106.875°-110.625°W, not the watershed boundary. A complete explanation of the merge technique is given in Appendix A. This 104-year rainfall index meets both our initial criteria (length, capturing most recent drought) for a record of Yaqui precipitation.

A number of additional climate datasets were used in our analysis. A yearly index of monsoon onset date, defined as the number of days after May 1st when rainfall exceeds 1 mm per day for five consecutive days, was calculated for the Yaqui region using daily rainfall data from the Zhu and Lettenmaier (2007) dataset averaged over the same region as our merged rainfall index. Global monthly SST anomaly fields were obtained from the current version of the Kaplan et al. (1998) gridded sea surface temperature anomaly (SSTA) dataset, which extends from 1856 though 2006. A "Gulf of California" SST index was calculated using the 1°-resolution Reynolds et al. (2002) optimally-interpolated (OI) SST dataset. Monthly indices for the Pacific Decadal Oscillation (PDO) (Mantua et al. 1997) and the Pacific-North American pattern (PNA) (Wallace and Gutzler 1981) were obtained from http://jisao.washington.edu/pdo/PDO.latest and http://jisao.washington.edu/data_sets/pna/, respectively. Otherwise, all SST indices used in this paper were constructed using the the Kaplan et al. SSTA product. Correlations between rainfall and a selection of relevant climate indices are shown in Table 1 and discussed in section 3.

Timeseries of inflow for each of the three large reservoirs in the Yaqui basin were provided by Mexico's Comisión Nacional del Agua (CNA). CNA calculates monthly inflow values as the open end of a water balance that takes into account measured reservoir releases, direct precipitation onto the reservoir, calculated evaporation, and measured changes in storage. Because known releases are

included in the water balance calculations, the inflow values are believed to provide a good estimate of natural flows within the basin (C.L. Addams, personal communication). The 47-year index of reservoir inflow (1956-2002) used in this study is a simple sum of the monthly inflow values from each of the three reservoirs.

Six standardized earlywood width chronologies from Douglas fir tree rings, which were used to create a multi-century reconstruction of wintertime rainfall for the Yaqui basin (see section 5c and Appendix B), are fully documented by Díaz et al. (2002).

3.   Climatology of Yaqui precipitation

In this section, we focus on basin-scale precipitation and the large-scale patterns of climatic variability associated with it at monthly and longer timescales. By averaging over space and time in this way, we minimize the difficulties associated with a sparse station network where daily records at individual stations may contain occasional gaps and measurement sites may change with time.

a.   *Annual cycle of precipitation*

Using our merged index, we find that the average annual precipitation for the Yaqui region is 552 mm with a yearly standard deviation of 102 mm. This arrives almost exclusively as rainfall; although portions of the watershed exceed 3000 m elevation in the Sierra Madre Occidental, even here, snowfall constitutes a negligible fraction of the annual total precipitation. The annual cycle of rainfall is shown in Figure 2. "Summer" (June-September or JJAS) rainfall dominates the annual total (394 mm or 71%) with most of the remainder (120 mm or 22%) falling during the "winter" (November-April or NDJFMA). The choice of NDJFMA for winter and JJAS for summer is based on the seasonal circulation regimes outlined below, a constraint imposed by a paleo-rainfall reconstruction discussed in section 4, and a desire for some separation (in this case one month) between seasons. Timeseries of seasonal and annual precipitation are shown in Figure 3. Note that, although the average summertime total is 3.5 times as large as the average wintertime total, the absolute variance for each season is approximately the same and the coefficient of variation is over three times as large for winter as it is for summer. As such, we have no *a priori* reason to expect a particular season to dominate in determining periods of meteorological drought.

Figure 4 shows the relationship between Yaqui precipitation and the global SST field on monthly and seasonal timescales, while Table 1 shows the correlation between Yaqui precipitation and a variety of climate indices of significance to the Pacific basin. Note that there is no significant correlation between summertime and wintertime precipitation ($r = -0.11$ for summer with the previous winter, $r = 0.15$ for winter with the previous summer), which allows us to discuss the precipitation regimes for each of these seasons in separate subsections below.

b.   *Summer (monsoon) regime*

Summertime precipitation is primarily associated with the North American Monsoon, which migrates up the Mexican west coast during the late spring, typically reaching the southern Yaqui watershed by the end of June. The Yaqui basin overlaps significantly with the area identified as "Monsoon South" through principal component analysis (PCA) by Comrie and Glenn (1998) and with the area identified as the "core" region of the North American Monsoon System by Gutzler (2004). Considerable effort, including an extensive recent field campaign (Higgins et al. 2006), has been devoted to understanding the precise mechanisms responsible for summer rainfall in this region but

little progress has been made toward identifying sources of seasonal predictability for summertime rainfall. In our analysis, we found no significant correlations between Yaqui rainfall and large-scale patterns of SST variability on either monthly or seasonal timescales for summer. Compositing shows that rainfall tends to be slightly higher ($\sim 6\%$) during ENSO-neutral summers than during summers when the average Nino3.4 Index (calculated as the mean SST anomaly over the Nino3.4 region, 5°S-5°N and 170°W-120°W) is more than 0.5°C above or below normal, but the scatter in summertime rainfall totals is quite large relative to this difference. Lorenz and Hartmann (2006) have suggested that, under appropriate conditions, eastward propagation of the Madden-Julian Oscillation across the Pacific can lead to surges of moisture into the Gulf of California that result in enhanced summertime rainfall over northwest Mexico; however, such events are not likely to be a source of predictability on timescales of a season or longer.

Zhu et al. (2007) have identified wintertime precipitation and antecedent soil moisture over northwest Mexico and the southwestern U.S. as possible determinants of monsoon onset date for this region; that is, greater winter/spring precipitation should lead to higher soil moisture, slower springtime land surface heating, and thus a delayed onset of monsoon rainfall. To test this hypothesis, we created indices for JFM, JFMA, and NDJFMA ("wintertime") precipitation by averaging 1901-1996 precipitation anomalies obtained from the Hulme et al. (1998) dataset over the region bounded by latitudes 28.75°N and 36.25°N and longitudes 106.875°W and 114.375°W, which corresponds as closely as possible to the winter/spring index region shown in Figure 7(a) of Zhu et al. (2007) given the gridspacing of the Hulme et al. data. When calculated for the entire 1901-1996 period, there is no statistically-significant correlation between any of these regional winter/spring precipitation indices and monsoon onset date in the Yaqui basin. We find, as Zhu et al. did, that periods of strong positive correlation between regional JFM (or JFMA) precipitation and monsoon onset date can be identified in the 1960s, 1970s, and 1980s with sliding correlation analysis using a 15-year window. However, the relationship is unstable (the correlation is actually negative prior to 1960) and we are unaware of any mechanism that might explain why such a relationship would hold only during certain periods and not others. Furthermore, the correlation between monsoon onset date and summertime total precipitation is not statistically significant through most of the 1960s, 1970s, and 1980s, and there appears to be no direct relationship between between summertime (JJAS) total rainfall in the Yaqui basin and regional rainfall during the previous winter ($r \approx -0.17$). Thus, while the possible impact of regional winter/spring precipitation on the timing and magnitude of the monsoon in northwest Mexico is certainly an interesting subject worthy of further research, we find that this mechanism offers little help in projecting summertime rainfall totals for the Yaqui basin.

Zhu et al. (2007) also found that land-sea temperature contrast plays a role in determining monsoon onset date and have suggested that variability in Gulf of California SSTs may play an important part in this relationship. If this were true, we would expect to find lower late spring SSTs during years of early monsoon onset; however, we find no significant correlation between May/June SSTs (either in the near-Pacific region or the Gulf of California itself) and monsoon onset in the Yaqui basin. In fact, for the period 1925-2004, summertime-total precipitation has a weak positive correlation ($r = 0.22$) with mean summertime SST in the near-Pacific region (110-120°W, 20-30°N). Analysis of cloud data from the International Satellite Cloud Climatology Project (ISCCP) for years 1984-2000 shows that above-normal summertime SSTs are associated with below-normal total cloud amount in this region. As such, we speculate that a more vigorous monsoon circulation during rainier summers *causes* the sea surface in the near-Pacific region to warm by forcing subsidence and clearing offshore.

c.   Winter (storm track) regime

Wintertime precipitation typically arrives in the Yaqui basin when the North Pacific storm track moves southward into the U.S. Southwest and northwest Mexico, producing peak precipitation in December. Aside from variations on synoptic timescales, which will not be discussed here, we suggest that the most important source of variability is that associated with sea surface temperature and winds in the equatorial Pacific. Other investigators have noted that the El Niño-Southern Oscillation (ENSO) serves to modulate the position and intensity of the North Pacific storm track (Trenberth et al. 1998, Seager et al. 2005). In particular, during the warm phase of ENSO (i.e. El Niño years), the subtropical wintertime jet intensifies and extends further eastward (Chang et al. 2002), bringing wet conditions to southern California, Arizona, New Mexico, and the northwestern Mexican states. Cleaveland et al. (2003) have documented the relationship between ENSO and rainfall for Durango, located southeast of the Yaqui basin, using both instrumental and reconstructed indices of precipitation.

We have found the total wintertime rainfall in the Yaqui region and a variety of wintertime-averaged indices of ENSO to be significantly correlated; the strongest relationship that we have identified is with the Nino3.4 Index ($r = 0.53$). Indeed, during El Niño winters (NDJFMA-average Nino3.4 Index more than $0.5°$C above normal) Yaqui rainfall averages 174 mm, while averaging only 81 mm during La Niña winters (NDJFMA-average Nino3.4 Index more than $0.5°$C below normal). Although Table 1 shows several other indices of variability that appear to be significantly correlated with Yaqui wintertime rainfall (regional SST, PDO, PNA), the statistical significance vanishes once any embedded ENSO-related signal is removed by linear regression from the index.

4.   Rainfall and reservoir storage

a.   Seasonal rainfall and reservoir inflow

To avoid the complexities and limitations associated with hydrological modeling, we take a simplistic approach and look for direct relationships between regional rainfall and reservoir inflow using a 47-year record of streamflow into the reservoir system provided by CNA. Throughout the year, rainfall is well correlated with inflow on a monthly basis ($r = 0.73$) but there are large seasonal differences: wintertime total rainfall is strongly correlated with wintertime total reservoir inflow ($r = 0.87$) while the correlation between summertime total rainfall and summertime total reservoir inflow is considerably weaker ($r = 0.59$). Furthermore, despite the fact that mean summertime-total inflow exceeds mean wintertime-total inflow (see Table 2), the variance in wintertime inflow is larger in both relative and absolute terms. A scatterplot of these data is shown in Figure 5. Note that the high wintertime correlation suggests that the impacts of evaporation (due to temperature and winds), changing land surface characteristics, vegetation, antecedent soil moisture, and any upstream withdrawals from the watershed (all of which may play a significant role in determining summertime streamflow totals) are small for this season. Wintertime total inflow is highly correlated with annual total inflow ($r = 0.80$), while summertime total inflow explains much less of the variance in the annual total ($r = 0.58$). The relationship between rainfall and reservoir inflow appears to be a stable one for the Yaqui basin: double-mass curve analysis of cumulative monthly reservoir inflow and cumulative monthly rainfall demonstrates a high level of stationarity, further suggesting that changes in upstream withdrawals, land use, and vegetation are relatively unimportant during the 1956-2002 period of record.

b.   Wintertime focus

Given that one of the goals of this study is the creation of a forecasting product useful for irrigation planning (to be discussed below), it makes sense to pause at this point and assess what types of forecasts might be possible. Considering the relationship with ENSO via modulation of the storm track, the strong connection between precipitation and reservoir inflow, and the strong variability in wintertime precipitation (as a fraction of the seasonal total), seasonal forecasts of wintertime reservoir inflow look like a promising possibility. However, prospects for summer are much less encouraging: variance in summertime reservoir inflow is much less (by a factor of 3/5) than it is for winter, we have been unable to identify any connections between summertime rainfall and large-scale patterns of variability, and summertime rainfall only explains a third of the variability in summertime reservoir inflow which, in turn, explains only a third of the variance in the annual total inflow. Other investigators have also found the summertime problem a vexing one for this region (e.g. Zhu et al. 2007). As such, we shall devote most of the remainder of this paper to the discussion of wintertime processes.

c.   Modeling reservoir inflow

The direct correlation between wintertime-average Nino3.4 Index and wintertime-total reservoir inflow ($r = 0.32$) is lower than, but not statistically distinct from, what would be expected given the individual ENSO-to-rainfall and rainfall-to-inflow correlations (estimated as the product of these correlations for the 1956-2002 period, $r \approx 0.47 \times 0.87 \approx 0.41$). Inflow totals for two winters (1968 and 1985) stand out as unusually large, and if data from these two years are withheld, the ENSO-to-inflow correlation rises to 0.59. However, given that rainfall was especially heavy during both of these winters (particularly in December), we cannot justify flagging these inflow values as statistical outliers. We find that a simple linear regression model provides an adequate description of the relationship between wintertime total reservoir inflow and wintertime-average Nino3.4 Index, as shown in Figure 6, although the model is rather sensitive to the particular subset of the data used for training. Including rainfall during the previous summer (a simple estimate of antecedent soil moisture) as a predictor variable provides no additional skill to the model. Using log-transform of reservoir inflow data also provides no additional skill.

5.   Drought in the Yaqui basin

a.   Defining drought

It appears that the term "drought" has no universally-accepted definition in the scientific literature (Wilhite and Glantz, 1985). Rather, it is described according to the quantity in deficit, a timescale (from weeks to centuries), and a particular assessment metric (e.g. the widely-used Palmer Drought Severity Index). In this study, we limit our attention to seasonal and annual *meteorological drought* on timescales of years to decades. For our purposes, a winter-season (summer-season, annual) drought is said to occur anytime the deficit in wintertime (summertime, annual) total precipitation, averaged over two or more successive years, exceeds a particular threshold. Other widely discussed types of drought include agricultural (deficits in soil moisture) and hydrological (deficits in runoff and streamflow). However, to the extent that Yaqui drought is caused primarily by wintertime climate anomalies, meteorological drought maps directly to hydrological drought due to the high correlation (0.87) between precipitation and streamflow in winter.

b. Drought in the historical (instrumental) record

Figure 3 shows seasonal and annual precipitation anomalies that have been treated with a six-year low-pass filter consisting of two successive passes of a three-year running mean. Prominent twentieth century droughts are easily seen, particularly in the annual total precipitation (bottom panel). Most apparent are the recent late-1990s/early-2000s drought and an especially severe drought that lasted through much of the 1950s. Less severe droughts also occurred in the early 1920s, mid-to-late-1930s, mid-1940s, and mid-1970s. It appears that Yaqui droughts can be associated with rainfall deficits in either season, although none of these droughts occurred in the absence of wintertime deficits and winter clearly dominates the annual precipitation signal (the seasonality of these droughts will be discussed in further detail below). Note also that 1980 through the early-1990s stands out as an anomalously wet period in this record.

Figure 3 indicates that most of the annual droughts during the 20th Century were associated with wintertime deficits. On interannual timescales, which are the most important for drought as it is treated in this paper, wintertime precipitation is much more strongly correlated with the annual total than is summertime precipitation on interannual timescales (e.g. $r = 0.82$ vs. $r = 0.58$ for data treated with a six-year lowpass filter), despite the fact that the correlations are indistinguishable ($r = 0.68$ vs. $r = 0.60$) for the unfiltered data. The most significant influence of large summertime deficits seems to have occurred in the 1950s, which, when combined with large wintertime deficits, gave rise to an especially long and severe drought. The sustained wintertime deficits for the periods 1950-57 and 1994-2002 are roughly the same, at ~ 41 mm/yr (34% of the mean wintertime total or 7% of the mean annual total), though the summertime deficits during the most recent drought were negligible.

Taking the instrumental period as typical, the recurrence frequency for summer and winter drought may be estimated and plotted, as in Figure 7. So far as the instrumental record is concerned, wintertime droughts appear to be more frequent and longer in duration than those due to summertime deficits, as suggested previously in Figure 3.

c. Rainfall reconstruction from tree rings

Although our merged index of Yaqui rainfall has proven useful for identifying the relationship between Yaqui rainfall and large-scale sources of variability, 104 years constitutes a relatively short record for obtaining good statistics on droughts that may last from several years to a decade or more. Given the scarcity of station data prior to the early 20th Century, the only alternative source of objective precipitation information would be a paleoclimate proxy for regional rainfall.

Using earlywood widths in Douglas fir cores obtained from sites in Chihuahua, Durango, and Texas, Díaz et al. (2002) have developed a long record of Chihuahua wintertime (NDJFMA) precipitation for the period 1647-1992. Although this record covers an area twice the size of that used for our merged Yaqui rainfall index (they use the two Hulme gridboxes that cover the Yaqui basin *and* the two gridboxes immediately to the east), it is well correlated ($r = 0.70$) with our wintertime-total rainfall index (described in section 2 and Appendix A) during the 1901-1992 overlap period. Díaz et al. produced their reconstruction by regressing the leading PC of standardized earlywood widths from six sites against wintertime rainfall totals obtained from the Hulme et al. dataset. As expected, this wintertime reconstruction is well correlated with ENSO. However, as a simple linear reconstruction, it fails to capture extreme events (especially the wettest winters) well during the overlap period and underestimates Yaqui-region rainfall because it also encompasses the drier region to the east of the Yaqui basin.

In an effort to better capture extreme events and also to provide a long timeseries more closely tied to precipitation in the Yaqui basin, we have produced a new wintertime rainfall reconstruction based on the same tree-ring data but using a slightly different methodology. For our reconstruction, the leading PC of standardized earlywood width *and the square of this PC* were regressed onto our merged Yaqui precipitation index. Our reconstructed precipitation index (1644-1992) is well correlated with our merged Yaqui basin precipitation index ($r = 0.71$) and with the Nino3.4 Index ($r = 0.57$). Cross-validation studies have demonstrated the stability of this reconstruction throughout the 1901-1992 overlap period. Although the increase in linear correlation with observed precipitation is not statistically significant, our reconstruction does a slightly better job of capturing extreme Yaqui precipitation events than the Díaz et al. reconstruction. See Appendix B for a further explanation of this reconstructed precipitation index.

d.   Wintertime drought in the paleo record

A timeseries of our wintertime rainfall reconstruction is plotted in Figure 8. Notable periods of wintertime drought include 1662-1678 (mean departure $= -45$ mm/y), 1702-1709 (-42 mm/y), 1728-1733 (-60 mm/y), 1772-1782 (-48 mm/y), 1785-1790 (-64 mm/y), 1857-1881 (-41 mm/y) encompassing the particularly dry period of 1859-1866 (-68 mm/y), and 1950-1957 (-67 mm/y), with all departures calculated relative to a 1901-1992 climatology that corresponds to the period of overlap with the instrumental record. This analysis suggests that severe droughts have occurred somewhat more frequently than estimated by the objective drought recurrence approach shown in Figure 7. Although trees may respond to moisture stress in a non-linear fashion and other variables may come into play, our reconstruction suggests that wintertime droughts at least as severe as the most recent one (1994-2002, 41 mm/winter mean deficit in our merged precipitation index) can be expected to recur about once every 50 years (7 severe droughts in 349 years). Thus, the fact that wintertime droughts of such severity have actually occurred twice in the past century is not surprising. Unfortunately, the lack of a suitable, long, summertime reconstruction makes it difficult to estimate recurrence times for summertime or annual droughts as severe as the 1950-1957 drought.

Some investigators have found paleoclimatic evidence for severe drought occurring synchronously over broad regions of the western United States and northern Mexico (Cook et al. 2004). Our rainfall reconstruction suggests that some wintertime droughts in the Yaqui basin may also occur independently of larger scale droughts that cover the western U.S. All three of the 19th-century North American droughts identified by Herweijer et al. (2006), including the so-called "Civil War drought" of 1856-1865, correspond to dry periods in our reconstruction. It appears that these events, as well as the widely-documented drought of the 1950s (e.g. Schubert et al. 2004), were associated with persistent La Niña-like conditions. However, fewer than half of the severe southwestern droughts identified in a reconstruction of Colorado river flow at Lee's Ferry, Arizona by Woodhouse et. al. (2006) correspond to periods of dryness in our Yaqui rainfall reconstruction during the 1644-1992 overlap interval, and the overall correlation between these two timeseries is quite weak ($r = 0.21$). This is unsurprising given that the correlation between wintertime precipitation in the region upstream of Lee's Ferry (as obtained from the Hulme et al. dataset) and wintertime rainfall in the Yaqui basin is $r < 0.4$. Furthermore, while the first two decades of the twentieth century stand out as the wettest period for the western United States during the past 1200 years (Woodhouse et al. 2005), the early twentieth century is merely one of several similarly wet periods in our reconstruction. Further analysis, and perhaps new paleoclimatic proxies, will be required to more fully understand how the causes of Yaqui drought (beyond modulation of wintertime precipitation by ENSO) relate to causes of large-scale drought in the western United States.

6. Predictability and forecasting

Next, we describe how the predictability of ENSO can be used along with the relationship between ENSO and Yaqui rainfall to generate seasonal projections of wintertime total rainfall in the Yaqui region. Although direct ENSO-to-reservoir forecasts might be more desirable from an end-user perspective, given the short reservoir record currently available and lack of stability demonstrated in our attempt to construct a simple linear model (see section 4c), the confidence in such forecasts would be relatively low.

a. ENSO forecasting

Over the past two decades, a variety of models have been developed for the prediction of SSTs in the the tropical Pacific, and more specifically, for the time evolution of the ENSO system. These range in complexity from simple persistence models to statistical/empirical models to fully-coupled ocean-atmosphere GCMs. Because tropical SSTs vary relatively slowly, the skill of persistence forecasts for monthly-mean ENSO indices is relatively good up to several months out. For longer lead times, the best empirical/statistical forecasts are as skillful as, but much less computationally expensive than, the best GCM-based forecasts. One category of empirical model, known as linear inverse models (LIMs), uses the time evolution of the leading modes of variability (EOFs) in tropical Pacific SSTs to project the future SST state (Penland and Magorian 1993). For our work, we used the results from a simple ensemble (that is, unweighted average) of seven ENSO models developed by Kirtman et al. (2001). Forecast skill is estimated as the correlation between the projected wintertime average Nino3.4 and the actual wintertime average Nino3.4 Index as derived from the Kaplan et al. (1998) SSTA dataset. For forecasts made up to two months in advance (i.e. based on June SST data), both persistence forecasts and the ensemble projection maintain high levels of skill ($r > 0.8$); however, for forecasts more than two months in advance, the ensemble forecasts do significantly better than persistence (e.g. $r \approx 0.83$ vs. $r \approx 0.32$ for April forecasts).

b. ENSO to precipitation forecasts

Using the significant correlation between the wintertime average Nino3.4 Index (or other ENSO indices) and wintertime total Yaqui rainfall, we develop a simple linear regression model for prediction of rainfall. We find rainfall (in mm) is related to the Nino3.4 Index (in °C) by the expression

$$P(t) = 45.3156\,N(t) + 121.6073,$$

which is plotted in Figure 9 along with training data for the period 1901-2004. Given a projected wintertime-average Nino3.4 value, a prediction for wintertime-total rainfall for the Yaqui region indicated by the dashed boxes in Figure 1 can be read directly from the plot. Cross-validation using randomly-chosen subsets of the available data show our model to be stable throughout the training period. In forecast mode, the Nino3.4 values used as input would either be derived from a single ENSO model (e.g. a Penland and Magorian-style LIM) or from an ensemble of ENSO models, and the expected skill would be estimated as the product of the ENSO forecast skill score and the skill of the ENSO-to-rainfall forecast, both of which are correlation coefficients. Table 3 shows estimated skill for ENSO forecasts based on persistence and the Kirtman et al. ensemble for a variety of lead times; also shown is the forecast skill for precipitation based on the best estimate of ENSO forecast skill (as a function of lead time). Although a forecast made 6 months out (at the end of April) can only be expected to explain 19% of the variance in wintertime Yaqui rainfall, such forecasts could provide a starting point for long range contingency planning in the Yaqui region.

In practical terms, a "deterministic" forecast such as that described above may be of limited utility given the relatively low skill level. Rather than a singular prediction of seasonal rainfall, it might be more useful to know the probability of the seasonal rainfall total lying within a particular range. Using 1901-2004 records of Yaqui wintertime total rainfall and the Nino3.4 Index, we calculate the frequency with which wet, normal, and dry conditions occurred for several ranges of the Nino3.4 Index. We defined "wet" as at least 20% above median wintertime rainfall (107 mm for the NDJFMA total) and "dry" as at least 20% below median wintertime rainfall, although these thresholds are arbitrary and precipitation terciles could be chosen to match the needs of agricultural planners; this $\pm 20\%$ threshold corresponds to a variation in wintertime-total reservoir inflow of $\pm 210 \times 10^6$ m^3 (30% of the wintertime median) by the regression relationship developed in section 4c. Nino3.4 categories were then automatically chosen such that equal numbers of realizations fell into each of the four categories. Represented graphically, as in Figure 10, the likelihood of wet, normal, or dry conditions can quickly be estimated given a projection of the wintertime average Nino3.4 Index. This forecasting approach could be readily adapted to a reservoir operations plan based on triggers: for each Nino3.4 category (i.e. vertical bar), a particular reservoir operations rule would be applied. Both methods could also be extended to give direct forecasts of wintertime total reservoir inflow for a given Nino3.4 projection, although it would be difficult to validate the models given the relatively short reservoir record.

7. Summary and conclusions

Mexico's Río Yaqui basin is a highly productive but climatologically vulnerable center of irrigation-dependent agriculture. Although over two thirds of the rainfall in this semi-arid region falls during the summer, wintertime rainfall is just as variable. Wintertime rainfall is well correlated with wintertime reservoir inflow which is, in turn, well correlated with annual total reservoir inflow. The corresponding relationships are much weaker during the summer and the overall variance in summertime inflow is also smaller than it is for winter.

While no sources of seasonal predictability have been identified for summertime rainfall, there is a strong positive correlation between wintertime rainfall and ENSO, which can be predicted with considerable skill many months in advance. Using these relationships we develop two simple statistical modeling approaches to leverage forecasts of ENSO indices for the projection of wintertime total rainfall and reservoir inflow.

Analysis of our 350-year tree-ring based reconstruction of wintertime rainfall shows that wintertime droughts as severe as the most recent drought occur, on average, about twice per century, which is consistent with the 20th century instrumental record. Such droughts are not always associated with broader regional droughts. Yaqui droughts of even greater severity than the most recent drought have occurred in the past and should be expected to occur in the future.

Appendix A: Construction of the merged Yaqui precipitation index

To create a monthly precipitation index representative of rainfall averaged over the Yaqui basin for the maximum possible duration, we chose to combine two gridded datasets of shorter duration, each ultimately based on station data. The Hulme et al. (1998) dataset, which contains monthly values at $3.75° \times 2.5°$ resolution for the period January 1900 through December 1996, was originally chosen because it had been used by Díaz et al. to train their tree-ring reconstruction of Chihuahua precipitation. Two of Hulme's gridboxes serve to cover most of the Yaqui watershed (see Figure 1). In order to capture the most recent drought, however, we needed to extend the Hulme dataset with more recent precipitation data. For this purpose we chose the all-Mexico dataset of Zhu and Lettenmaier (2007), which provides daily precipitation totals at $1/8° \times 1/8°$ resolution for the period 1 January 1925 through 31 October 2004 and was originally developed for use with a hydrological model.

The merged precipitation index was created as follows. First, a Hulme-based monthly index for the period October 1900 through September 1996 (water years 1901-1996) was created by averaging the two Hulme gridboxes that cover the Yaqui basin. Next, the daily data in the Zhu-Lettenmaier dataset was averaged over the area corresponding to the two Hulme gridboxes into a monthly index for the period October 1939 through September 2004 (water years 1940-2004); data prior to water year 1940 was rejected based on the recommendation of Zhu (personal communication) that the earlier data in the record was somewhat less reliable. It was found that these two indices were nearly identical during the October 1939 through September 1996 overlap period, with a correlation coefficient of $r = 0.97$, although the variance (about the climatological annual cycle) in the Zhu-Lettenmaier index was somewhat smaller than than that of the Hulme index during the overlap period. Next, the annual cycle as calculated from the Zhu-Lettenmaier-based index during the overlap period was subtracted from the October 1995 through September 2004 data from the same index. This anomaly timeseries was then scaled by the ratio of the standard deviations of the two timeseries during the overlap period and added to the annual cycle during the overlap period as calculated from the Hulme-based index. Finally, this nine-year extension was appended to the Hulme-based index, creating a monthly index of Yaqui precipitation for water years 1901-2004.

Appendix B: Creation and validation of the tree-ring based rainfall index

In recent years, there has been an impressive and successful effort to reconstruct precipitation in northwest Mexico using tree rings; Villanueva-Díaz et al. (2006) provides a good overview of much of this work. Of particular interest for the present study is a 1647-1992 tree-ring based reconstruction of Chihuahua wintertime rainfall by Díaz et al. that is well correlated with Yaqui rainfall during the 1901-1992 instrumental period and with indices of ENSO. However, this reconstruction is valid for a region that is both larger (encompassing two additional Hulme gridboxes to the east of the Yaqui basin) and, on average, drier than the Yaqui basin. Furthermore, the reconstruction captures only 34% of the variance seen in our Yaqui wintertime precipitation index during the period of overlap and misses a number of extreme precipitation events. As such, this reconstruction was not entirely appropriate for the purposes of our study.

Still, given that the individual tree-ring chronologies produced by Díaz et al. are better correlated with Yaqui wintertime rainfall than any others located in this region, their work serves as a useful starting point. To customize this data, we chose to calculate our own tree-ring based rainfall reconstruction with a modified version of the Díaz et al. method, which used a linear least squares fit of the PC associated with the first EOF of standardized Douglas fir earlywood ringwidth from the six measurement sites with precipitation averaged over all of Chihuahua (as represented by the

average of four Hulme et al. gridboxes that approximately cover this area). Instead, we used multiple linear regression of the first PC *and its square* with the wintertime-total (NDJFMA) precipitation obtained from our merged Yaqui precipitation index (i.e. the "instrumental record"). Von Storch et al. (2004) have noted that significant loss of variance is an endemic problem with regression-based reconstructions; in particular, it would complicate the threshold-based approach to drought identification we have employed in this study. To avoid this difficulty, the resulting 349-year timeseries was scaled to the variance of the instrumental record by multiplying it by the ratio of the standard deviations of the two timeseries during the 1901-1992 overlap period, following the method of Cook et al. (2004). Cross-validation was performed by repeatedly withholding a randomly-chosen fourth (23 years) of the rainfall data, training the reconstruction on the remaining data, and then verifying the reconstruction model on the withheld data. Using this method, the model was found to be quite stable. The overall correlation between our merged Yaqui precipitation index and our quadratic tree-ring reconstruction (the final version of which was produced using data from the entire 1901-1992 period) is $r = 0.71$. Although this correlation represents no statistically significant improvement over the Díaz et al. dataset, Figure 11 shows that our reconstruction does offer some improvement in the capture of extreme events.

REFERENCES

Addams, C.L., 2004: Water policy evaluation using a combined hydrological-economic-agronomic modeling framework: Yaqui Valley, Sonora, Mexico. Dissertation, Stanford University, 354 pp.

Chang, E.K.M., S. Lee, and K.L. Swanson, 2002: Storm Track Dynamics. *J. Climate.* **15**, 2163-2183.

Cleaveland, M.K., D.W. Stahle, M.D. Therrell, J. Villanueva-Díaz, and B.T. Burns, 2003: Tree-ring reconstructed winter precipitation and tropical teleconnections in Durango, Mexico. *Climatic Change*, **59**, 369-388.

Comrie, A.C. and E.K. Glenn, 1998: Principal components-based regionalization of precipitation regimes across the southwest United States and northern Mexico, with an application to monsoon precipitation variability. *Climate Res.*, **10**, 201-215.

Cook, E.R., C.A. Woodhouse, C.M. Eakin, D.M. Meko, and D.W. Stahle, 2004: Long-term aridity changes in the western United States. *Science*, **306**, 1015-1018. [Online supporting material at http://www.sciencemag.org/cgi/content/full/1102586/DC1.]

Díaz, S.C., M.D. Therrell, D.W. Stahle, and M.K. Cleaveland, 2002: Chihuahua (Mexico) winter-spring precipitation reconstructed from tree-rings, 1647-1992. *Climate Res.*, **22**, 237-244.

Fischer, R.A., 1985: Number of kernels in wheat crops and the influence of solar radiation and temperature. *J. Agricultural Sci.*, **105**, 447-461.

Gutzler, D.S., 2004: An index of interannual precipitation variability in the core of the North American monsoon region. *J. Climate*, **17**, 4473-4480.

Herweijer, C., R. Seager, and E.R. Cook, 2006: North American droughts of the mid to late nineteenth century: a history, simulation and implication for Mediaeval drought. *The Holocene*, **16**, 159-171.

Higgins, W., D. Ahijevych, J. Amador, A. Barros, E.H. Berbery, E. Caetano, R. Carbone, P. Ciesielski, R. Cifelli, M. Cortez-Vazquez, A. Douglas, M. Douglas, G. Emmanuel, C. Fairall, D. Gochis, D. Gutzler, T. Jackson, R. Johnson, C. King, T. Lang, M.-I. Lee, D. Lettenmaier, R. Lobato, V. Magaña, J. Meiten, K. Mo, S. Nesbitt, F. Ocampo-Torres, E. Pytlak, P. Rogers, S. Rutledge, J. Schemm, S. Schubert, A. White, C. Williams, A. Wood, R. Zamora, and C. Zhang, 2006: The NAME 2004 field campaign and modeling strategy. *Bull. Amer. Meteor. Soc.*, **87**, 79-94.

Hulme, M., T.J. Osborn, and T.C. Johns, 1998: Precipitation sensitivity to global warming: Comparison of observations with HadCM2 simulations. *Geophys. Res. Lett.*, **25**, 3379-3382.

Kaplan, A., M. Cane, Y. Kushnir, A. Clement, M. Blumenthal, and B. Rajagopalan, 1998: Analyses of global sea surface temperature 1856-1991. *J. Geophys. Res.*, **103**, 18,567-18,589.

Kirtman, B.P., J. Shukla, M. Balmaseda, N. Graham, C. Penland, Y. Xue, and S. Zebiak, 2001: Current Status of ENSO Forecast Skill: A Report to the CLIVAR Working Group on Seasonal to Interannual Prediction. WCRP Informal Report No. 23/01, ICPO Publication No. 56, World Climate Research Programme, 26 pp.

Lobell, D.B., J.I. Ortiz-Monasterio, G.P. Asner, R.L. Naylor, and W.P. Falcon, 2005a: Combining field surveys, remote sensing, and regression trees to understand yield variations in an irrigated wheat landscape. *Agronomy J.*, **97**, 241-249.

Lobell, D.B., J.I. Ortiz-Monasterio, G.P. Asner, P.A. Matson, R.L. Naylor, and W.P. Falcon, 2005b: Analysis of wheat yield and climatic trends in Mexico. *Field Crops Res.*, **94**, 250-256.

Lorenz, D.J. and D.L. Hartmann, 2006: The effect of the MJO on the North American Monsoon. *J. Climate*, **19**, 333-343.

Mantua, N.J., S.R. Hare, Y. Zhang, J.M. Wallace, and R.C. Francis, 1997: A Pacific interdecadal climate oscillation with impacts on salmon production. *Bull. Amer. Meteor. Soc.*, **78**, 1069-1079.

McCullough, E., 2005: Coping with Drought: An Analysis of Crisis Responses in the Yaqui Valley. Thesis, Earth Systems Program, Stanford University, 71 pp.

Penland, C. and T. Magorian, 1993: Prediction of Niño 3 sea surface temperatures using linear inverse modeling. *J. Climate*, **6**, 1067-1076.

Reynolds, R.W., N.A. Rayner, T.M. Smith, D.C. Stokes, and W. Wang, 2002: An improved in situ and satellite SST analysis for climate. *J. Climate*, **15**, 1609-1625.

Seager, R., N. Harnik, W.A. Robinson, Y. Kushnir, M. Ting, H.-P. Huang, and J. Velez, 2005: Mechanisms of ENSO-forcing of hemispherically symmetric precipitation variability. *Quart. J. Roy. Meteor. Soc.*, **131**, 1501-1527.

Schubert, S.D., M.J. Suarez, P.J. Pegion, R.D. Koster, and J.T. Bacmeister, 2004: Causes of long-term drought in the U.S. Great Plains. *J. Climate*, **17**, 485-503.

Trenberth, K.E., G.W. Branstator, D. Karoly, A. Kumar, N.-C. Lau, and C. Ropelewski, 1998: Progress during TOGA in understanding and modeling global teleconnections associated with tropical sea surface temperatures. *J. Geophys. Res.*, **103**, 14,291-14,324.

Villanueva-Díaz, J., J.C. Paredes, B.H. Luckman, J.E. Ávalos, D.W. Stahle, I.S. Cohen, M.D. Therrell, and R.M. Martínez, 2006: *Precipitación y Flujo Histórico de la Cuenca Nazas-Aguanaval e Impaco en la Agricultura.* Instituto Nacional de Investigaciones Forestales, Agrícolas y Pecuarias (México), 44 pp.

von Storch, H., E. Zorita, J.M. Jones, Y. Dimitriev, F. González-Rouco, and S.F.B. Tett, 2004: Reconstructing Past Climate from Noisy Data. *Science*, **306**, 679-682.

Wallace, J.M. and D.S. Gutzler, 1981: Teleconnections in the geopotential height field during the Northern Hemisphere winter. *Mon. Wea. Rev.*, **109**, 784-812.

Wilhite, D.A. and M.H. Glantz, 1985: Understanding the Drought Phenomenon: The Role of Definitions. *Water International*, **10**, 111-120.

Woodhouse, C.A., K.E. Kunkel, David R. Easterling, and E.R. Cook, 2005: The twentieth-century pluvial in the western United States. *Geophys. Res. Lett.*, **32**, 1-4.

Woodhouse, C.A., S.T. Gray, and D.M. Meko, 2006: Updated streamflow reconstructions for the Upper Colorado River Basin. *Water Resour. Res.*, **42**, 1-16.

World Resources Institute, cited 2006: Yaqui Watershed. [Available online at http://pdf.wri.org/watersheds_2000/watersheds_namerica_p2_138.pdf.]

Zhu, C. and D.P. Lettenmaier, 2007: Long-term climate and derived surface hydrology and energy flux data for Mexico, 1925-2004. *J. Climate* **20**, 1936-1946.

Zhu, C., T. Cavazos, and D.P. Lettenmaier, 2007: Role of antecedent land surface conditions in warm season precipitation over northwest Mexico. *J. Climate* **20**, 1774-1791.
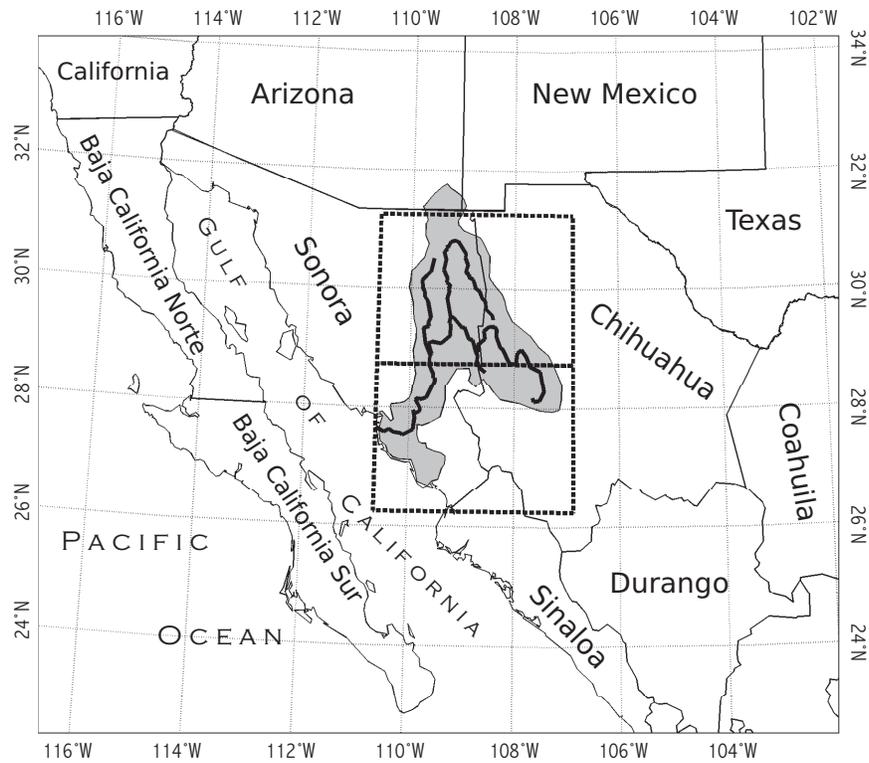
Figure 1: Location of the Río Yaqui watershed (gray shading) in northwest Mexico. Dashed outline boxes indicate the locations of the two Hulme et al. (1998) gridboxes from which data was used in creating our merged precipitation index for the Yaqui region.
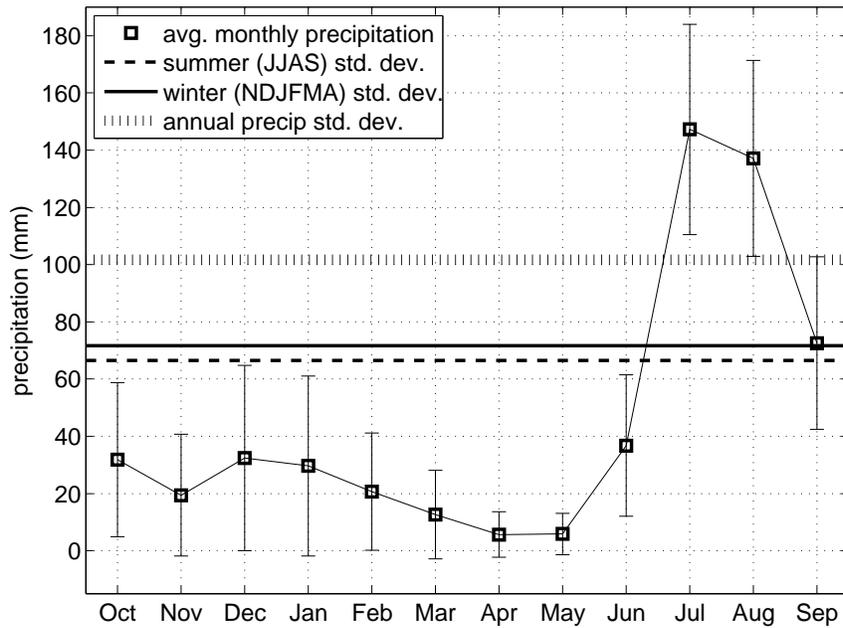

Figure 2: Annual cycle of rainfall in the Yaqui basin based on water year 1901-2004 data. Bars indicate monthly standard deviations; horizontal lines indicate standard deviations for seasonal and annual precipitation totals.
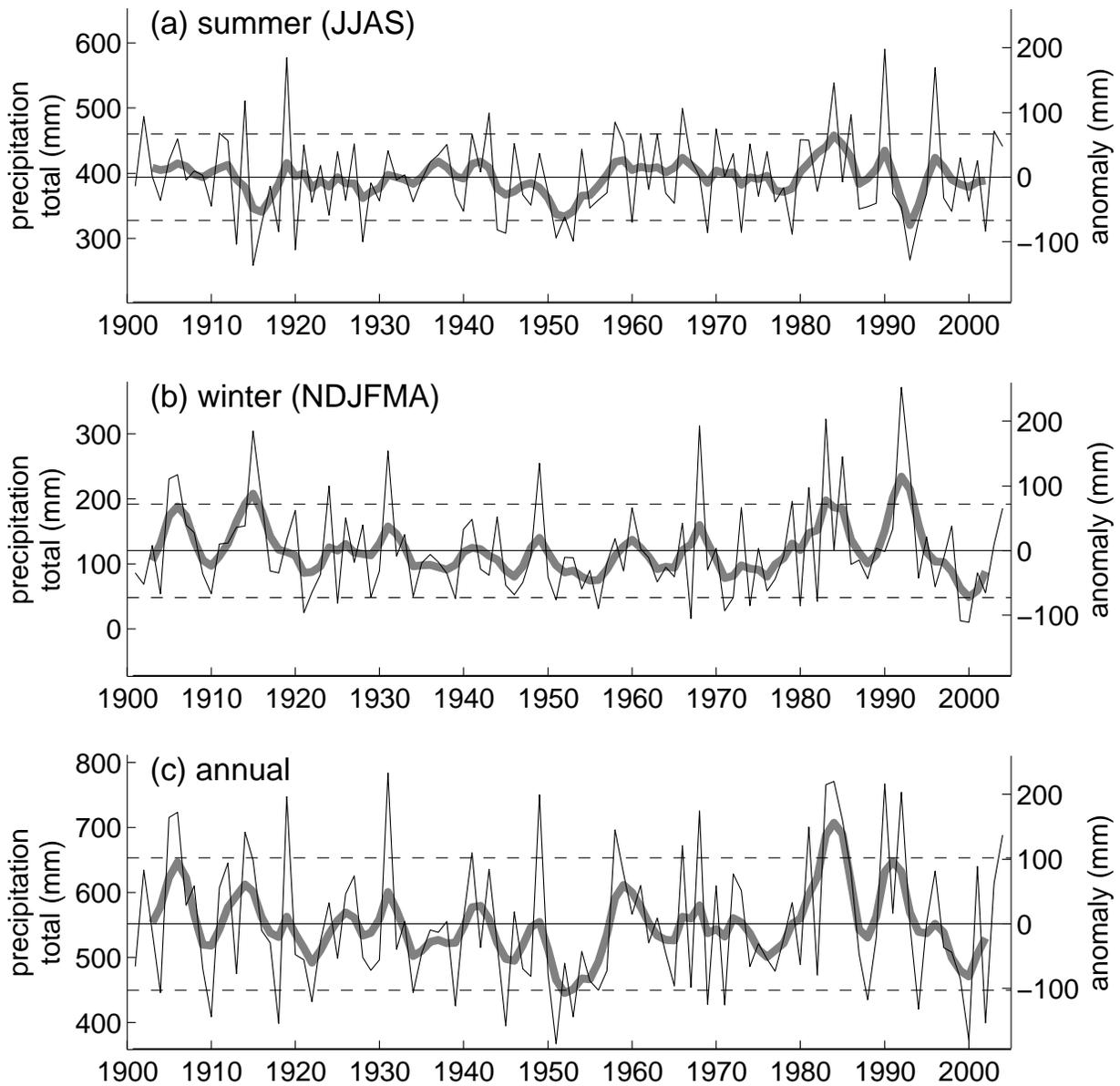
Figure 3: Summer-season, winter-season, and annual precipitation totals in the Yaqui basin for water years 1901-2004 (thin black lines) overlaid on lowpass-filtered versions of the same timeseries (wider gray lines); anomalies relative to the entire period are indicated on the right vertical axis. Dashed lines indicate plus and minus one standard deviation for the summer (66 mm), winter (72 mm), and annual (102 mm) totals. The filtered timeseries were created by processing the unfiltered anomalies with two successive passes of a three-year running mean. Note that the three plots are shown at the same scale to facilitate comparison.
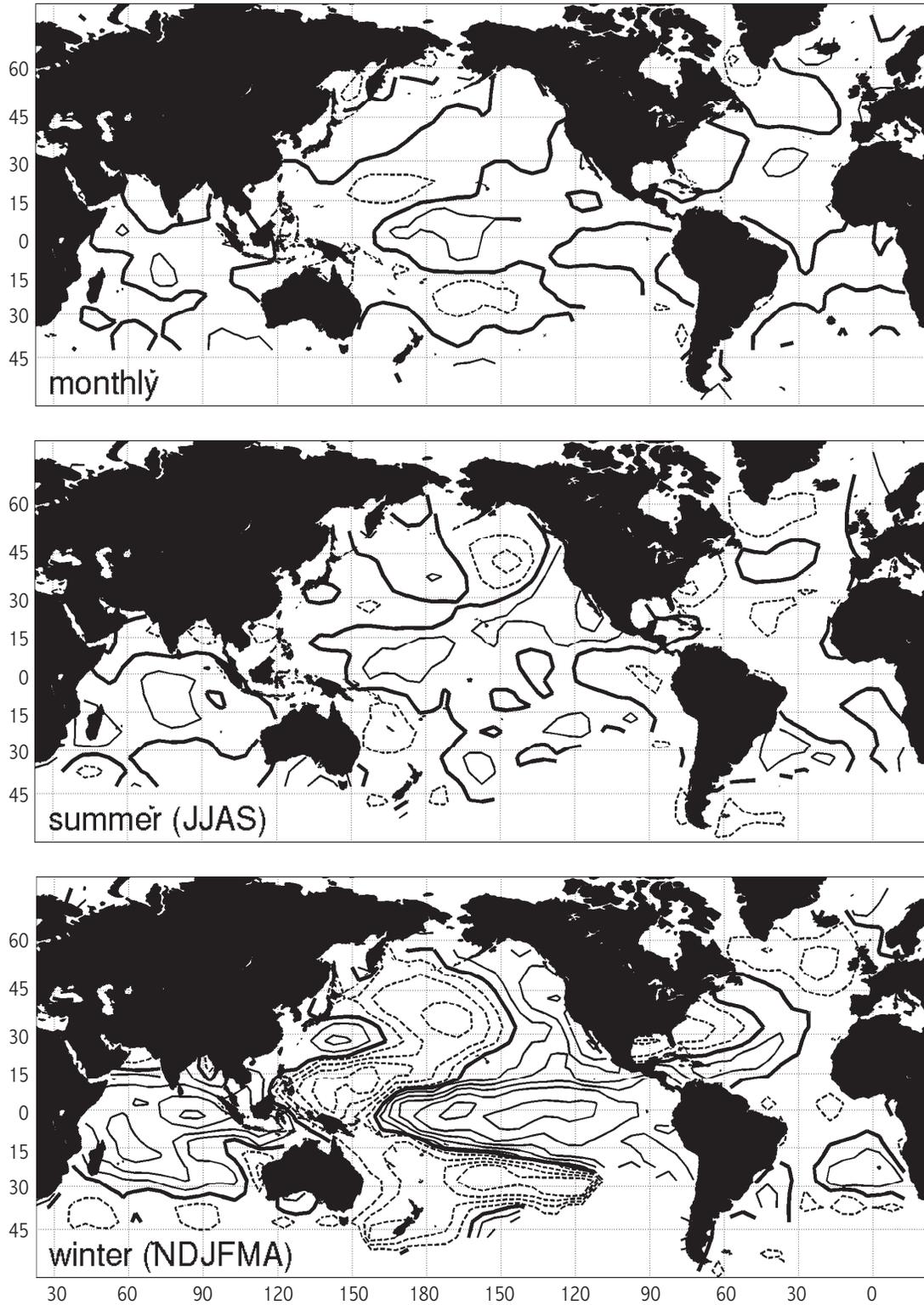
Figure 4: Correlation of Yaqui total precipitation with local average SST on monthly and season-averaged timescales for water years 1901-2004. The contour interval is 0.1 with positive correlations shown as solid lines, negative correlations shown as dashed lines, and the zero contour drawn in bold.
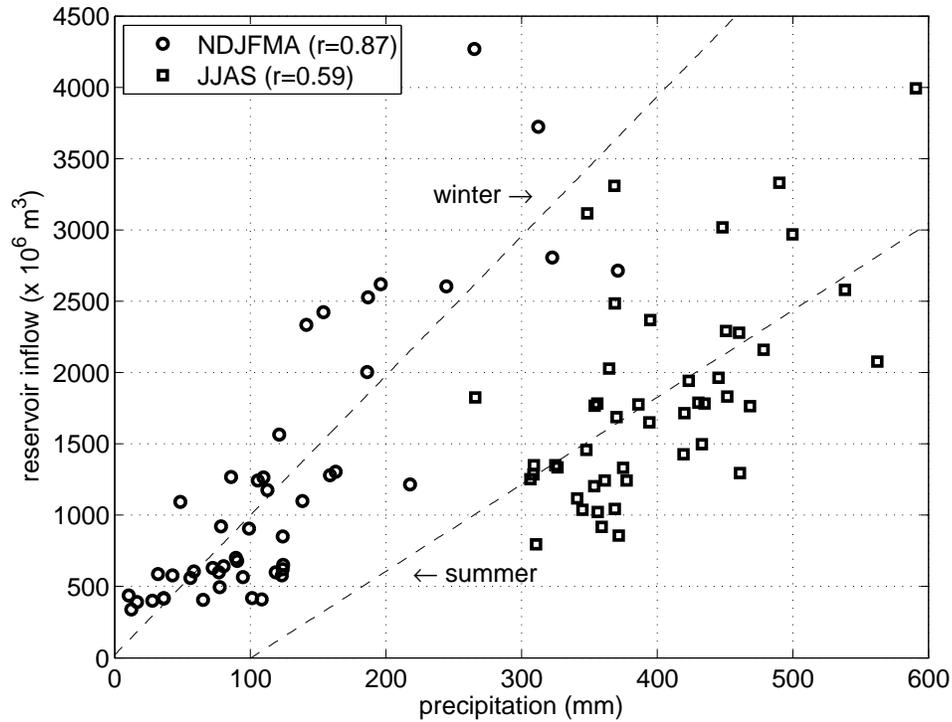
Figure 5: Seasonal precipitation and reservoir inflow in the Yaqui basin for the period 1956-2002. Dashed lines indicate the best-fit linear relationship between rainfall and inflow.
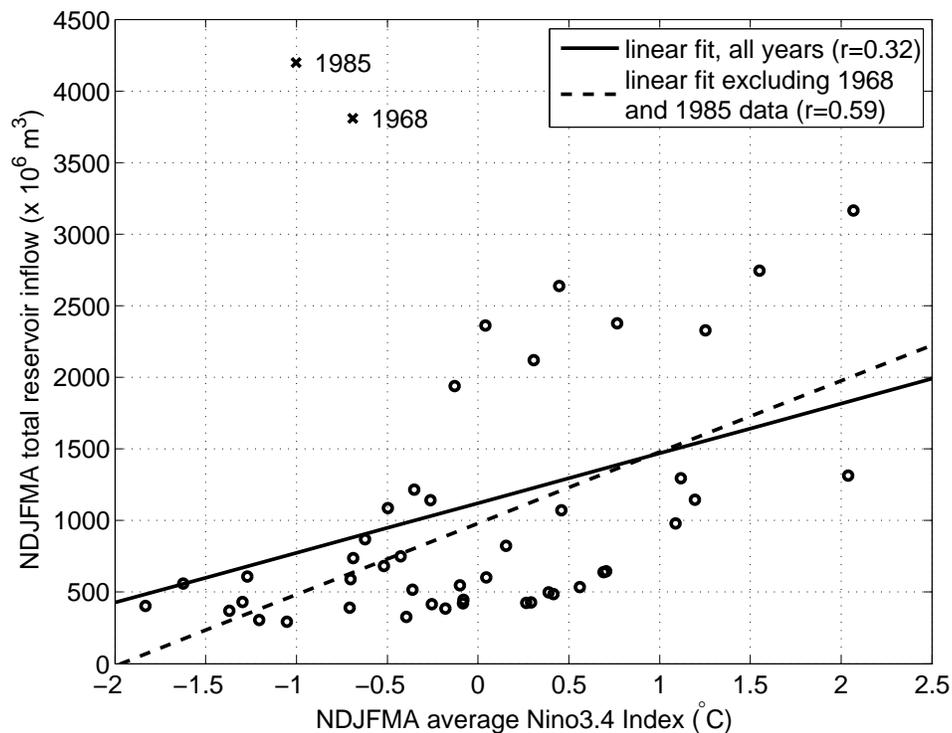

Figure 6: Wintertime-average Nino3.4 Index and wintertime-total reservoir inflow in the Yaqui basin for the period 1956-2002. The solid line shows the best-fit linear relationship between ENSO and inflow using all available data. The dashed line shows the relationship obtained if data from from two years with unusually large inflow values (1968 and 1985, plotted with the symbol ×) are excluded from the analysis.
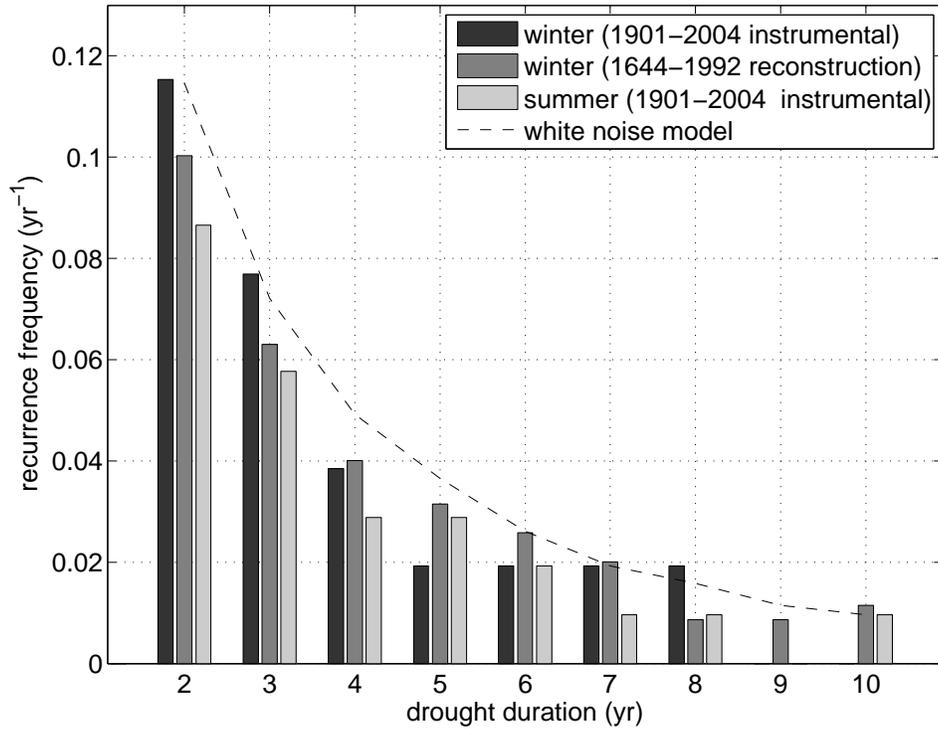
Figure 7: Seasonal drought recurrence frequency in the instrumental record and our tree-ring based reconstruction. A drought of length n years is said to occur when the average deficit for the n years exceeds 41 mm/yr, which was the average wintertime deficit during the recent 1994-2002 drought and represents a 34% (10%) reduction in the climatologically-averaged wintertime (summertime) total rainfall.
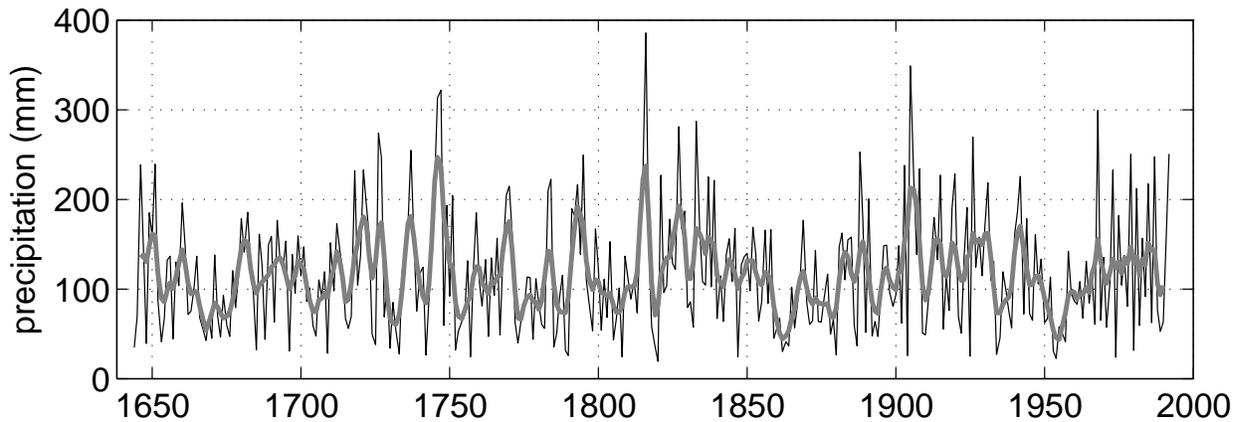

Figure 8: Timeseries of our tree-ring based reconstruction of wintertime-total precipitation for the Yaqui region for the period 1644-1992 (thin black) overlaid on a lowpass-filtered version of this reconstruction (thick gray).
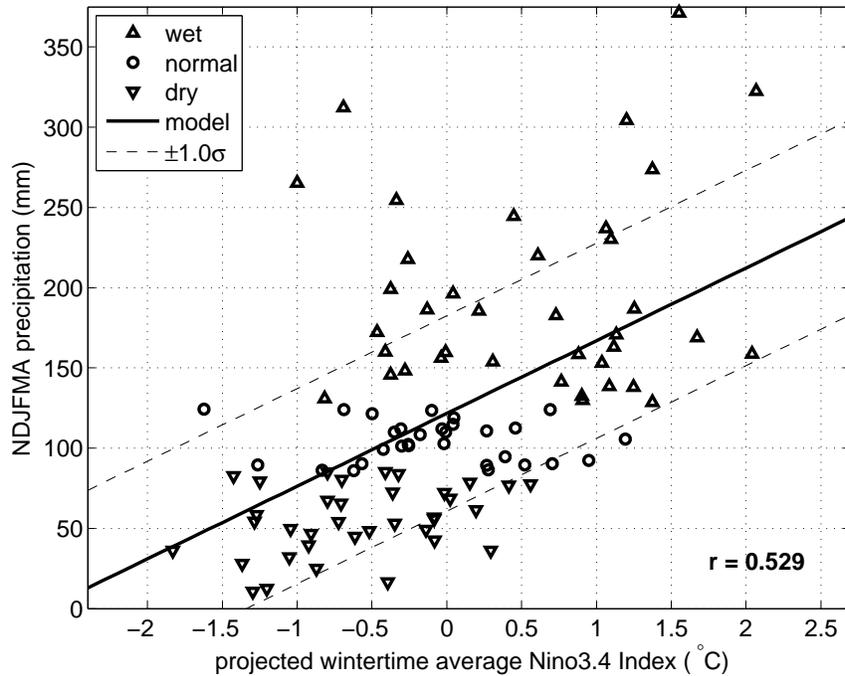
Figure 9: Linear regression model for projection of wintertime total rainfall from a known or predicted wintertime average Nino3.4 Index. Wintertime total rainfall is considered "normal" if it falls within 20% (21 mm) of the median value (107 mm).
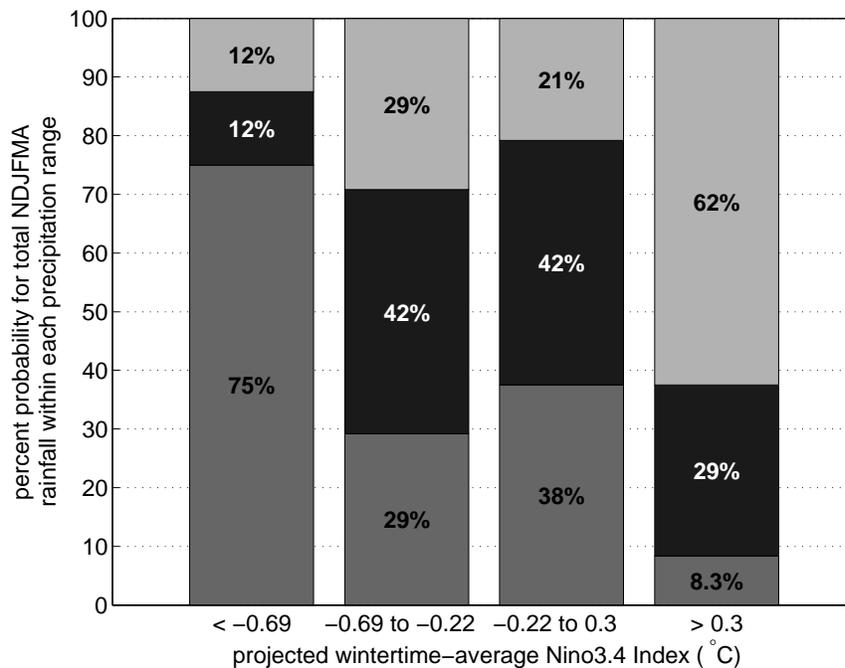

Figure 10: Probability of wet (light gray, top), normal (dark gray, middle), and dry (medium gray, bottom) winters for four different ranges of the wintertime average Nino3.4 Index. Rainfall is considered "normal" if it falls within 20% (21 mm) of the median value (107 mm). Each bar represents 26 years of data.
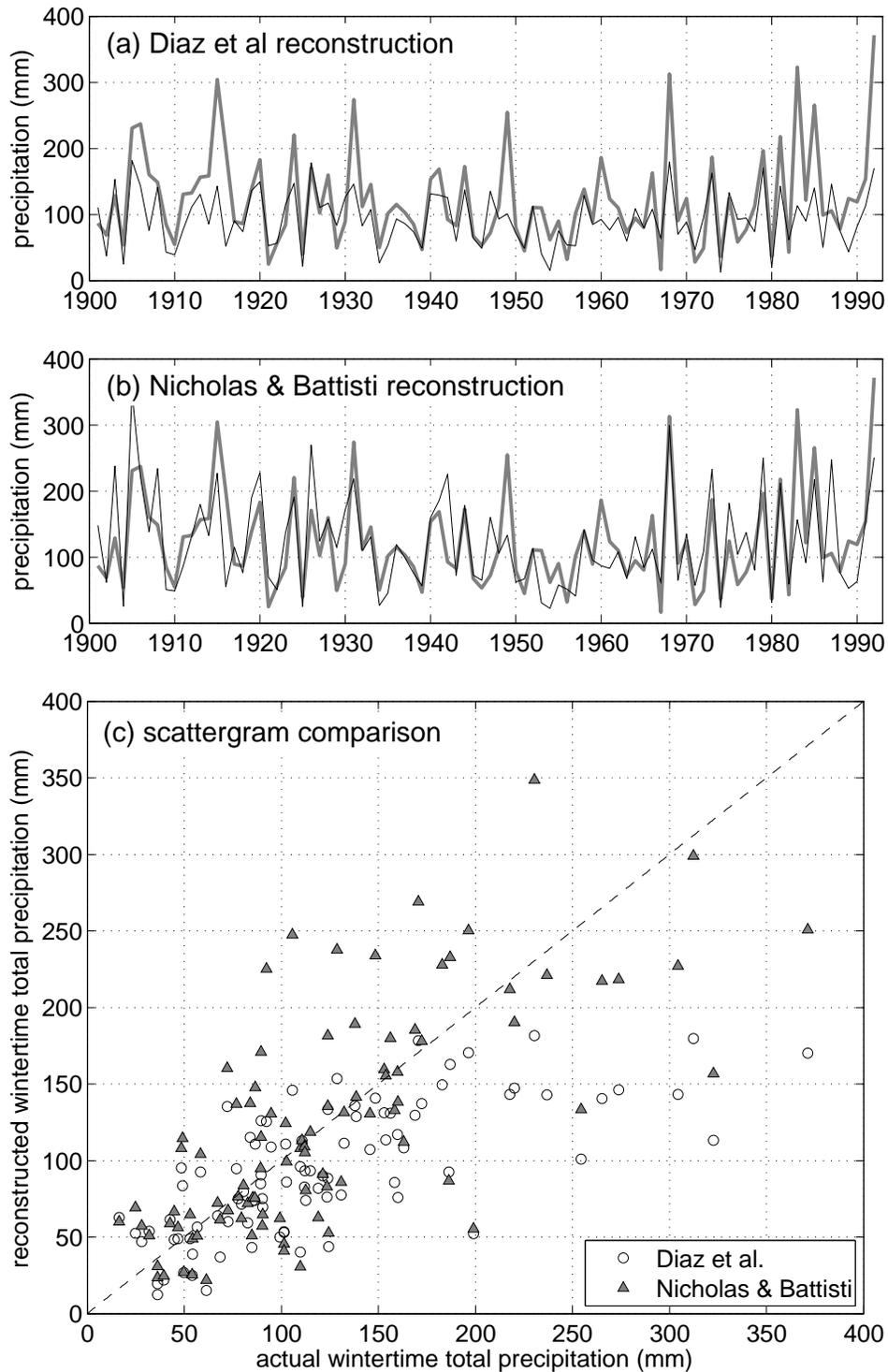
Figure 11: Two tree-ring based reconstructions of rainfall compared to observed Yaqui wintertime (NDJFMA) rainfall for the period 1901-1992. Both reconstructions are derived from the same standardized Douglas fir earlywood widths. (a) The Díaz et al. reconstruction (black) and observed precipitation (gray). (b) Our reconstruction (black) and observed precipitation (gray). (c) Scattergram comparison of the two reconstructions with observed precipitation; a dashed line of slope one has been added for reference.

Table 1: Correlation of Yaqui precipitation totals with various climate indices averaged for the interval/season indicated. "Regional SST" is computed by averaging the Kaplan et al. SST anomalies (5° resolution) over the area bounded by 110-120°W and 20-30°N, which corresponds to the region of high summertime rainfall-SST correlations near Baja California in Figure 4. "Gulf of CA SST" is computed by averaging the Reynolds et al. (2002) SSTs (1° resolution) over the Gulf of California. ENSO indices are computed from the Kaplan et al. SST anomalies. Values for the Pacific Decadal Oscillation (PDO) index (Mantua et al. 1997) were obtained from http://jisao.washington.edu/pdo/PDO.latest; values for the Pacific-North American pattern (Wallace and Gutzler 1981) index were obtained from http://www.jisao.washington.edu/data_sets/pna/. All indices based on data for water years 1901-2004 except for Gulf of California SST (1982-2004) and the PNA index (1949-2004). Correlations significant at the 95% confidence level ($p = 0.05$) are printed in bold type.

season	global SST	regional SST	Gulf of CA SST	Nino1+2 Index	Nino3 Index	Nino3.4 Index	Nino4 Index	PDO Index	PNA Index
monthly	0.02	0.06	0.08	−0.01	0.01	0.08	0.12	0.01	0.01
winter	0.10	**0.39**	0.38	**0.40**	**0.51**	**0.53**	**0.48**	**0.27**	**0.29**
summer	−0.01	**0.22**	0.22	−0.09	−0.04	0.02	**0.07**	0.05	−0.03
annual	0.11	**0.39**	0.37	**0.20**	**0.35**	**0.39**	**0.39**	**0.33**	0.20

Table 2: Average total inflow for the three major reservoirs in the Yaqui basin, 1956-2002.

	average total inflow ($\times 10^9$ m^3)	variance ($\times 10^{18}$ m^6)
summer	1.816	0.524
winter	1.108	0.940
annual	3.142	1.573

Table 3: Skill (in a correlation sense) for forecasts of wintertime-average (NDJFMA) Nino3.4 Index and wintertime-total rainfall in the Yaqui basin. "Ensemble mean" skill scores are estimated based on Figure 3 of Kirtman et al. (2001).

lead time (months)	forecast made at the end of	ENSO forecast skill using persistence	ENSO forecast skill using ensemble mean	best estimate Yaqui rainfall forecast skill
0	October	0.91	0.86	0.48
1	September	0.86	0.88	0.47
2	August	0.83	0.88	0.47
3	July	0.75	0.88	0.47
4	June	0.69	0.90	0.48
5	May	0.51	0.88	0.47
6	April	0.32	0.83	0.44